Linear element formation and their role in meiotic sister chromatid cohesion and chromosome pairing

Monika Molnar[1], Eveline Doll[2], Ayumu Yamamoto[1], Yasushi Hiraoka[1,*] and Jürg Kohli[2]

[1]CREST Research Project, Kansai Advanced Research Center, Communications Research Laboratory, Kobe 651-2492, Japan
[2]Institute of Cell Biology, University of Bern, CH-3012 Bern, Switzerland
*Author for correspondence (e-mail: yasushi@crl.go.jp)

Accepted 23 January 2003
Journal of Cell Science 116, 1719-1731 © 2003 The Company of Biologists Ltd
doi:10.1242/jcs.00387

Summary

Fission yeast does not form synaptonemal complexes in meiotic prophase. Instead, linear elements appear that resemble the axial cores of other eukaryotes. They have been proposed to be minimal structures necessary for proper meiotic chromosome functions. We examined linear element formation in meiotic recombination deficient mutants. The *rec12*, *rec14* and *meu13* mutants showed altered linear element formation. Examination of *rec12* and other mutants deficient in the initiation of meiotic recombination revealed that occurrence of meiosis-specific DNA breaks is not a precondition for the formation of linear elements. The *rec11* and *rec8* mutants exhibited strongly impaired linear elements with morphologies specific for these meiotic cohesin mutants. The *rec10* and *rec16/rep1* mutants lack linear elements completely. The region specificity of loss of recombination in the *rec8*, *rec10* and *rec11* mutants can be explained by their defects in linear element formation. Investigation of the *rec10* mutant showed that linear elements are basically dispensable for sister chromatid cohesion, but contribute to full level pairing of homologous chromosomes.

Key words: Meiosis, Fission yeast, Linear elements, Sister chromatid cohesion, Homologous chromosome pairing

Introduction

In the life cycle of sexually reproducing organisms meiosis halves the chromosome number in the germ line cells and produces haploid gametes. This halving is achieved by two consecutive divisions following a single round of DNA replication. The second (equational) division resembles mitotis: sister chromatids segregate into daughter nuclei. However, the first (reductional) division has unique features. During the first meiotic division homologous chromosomes pair, undergo high levels of recombination, and the resulting chiasma formation assists their segregation into daughter nuclei. In most organisms, pairing of homologous chromosomes in meiotic prophase is accompanied by the formation of synaptonemal complexes (SC). The synaptonemal complex is an evolutionary well-conserved, strictly meiosis specific, proteinaceous structure. In early prophase, after DNA replication axial elements (AE) start to connect the sister chromatids. By the pachytene stage of meiotic prophase, chromosome pairing and synaptonemal complex development culminate in the formation of a tripartite structure: the axial elements (now called lateral elements, LE) are connected by a central component (for reviews, see Zickler and Kleckner, 1999; Roeder, 1997; Kleckner, 1996).

The fission yeast *Schizosaccharomyces pombe* is a haploid, unicellular eukaryote. Naturally, *S. pombe* cells undergo meiosis directly after mating of two cells of opposite mating-type (zygotic meiosis). However, diploid cells heterozygous for mating-type can be maintained, and synchronous meiosis can be induced by shifting the culture to nitrogen-free medium (azygotic meiosis) (Egel, 1973; Egel and Egel-Mitani, 1974). Meiosis in fission yeast has unusual features. In prophase, the meiotic nucleus oscillates between the cell poles (Chikashige et al., 1994). These movements confer an elongated shape to the nucleus [horse-tail nucleus (Robinow, 1977)], and are led by the SPB and the attached telomere cluster (Chikashige et al., 1994; Chikashige et al., 1997). Thus, the bouquet structure of chromosomes bundled at the telomeres is maintained during the whole meiotic prophase in fission yeast. Homologous chromosome pairing and recombination occur during horse-tail movements. Mutants impaired in telomere clustering or nuclear movement show decreased homologous pairing and recombination, indicating the importance of these events in homolog juxtaposition (Shimanuki et al., 1997; Cooper et al., 1998; Nimmo et al., 1998; Yamamoto et al., 1999). Fission yeast is highly proficient in meiotic recombination but shows no crossover interference (Munz, 1994).

It has been long known that fission yeast does not form synaptonemal complexes. Instead, filamentous structures (linear elements) appear in meiotic prophase. They resemble the axial cores of other eukaryotes (Olson et al., 1978; Hirata and Tanaka, 1982). The adaptation of the nuclear spreading technique to fission yeast made possible a detailed analysis of linear element formation in meiotic time-course experiments (Bähler et al., 1993). Linear elements do not form continuously along the chromosomes and undergo morphological changes during meiotic prophase. Bähler et al. have proposed that the organization of chromatin in the linear elements may facilitate meiotic chromosome functions, such as sister chromatid cohesion, chiasma maintenance, homologous pairing and the resolution of interlocks (Bähler et al., 1993). Analysis of the *rec8-110* mutant revealed coincidence of impairment of linear element formation, precocious sister chromatid separation, and

Table 1. Strains used in this study

Strain	Genotype
JB6	*h⁺/h⁻ ade6-M210/ade6-M216*
ED1	*h⁺/h⁻ rec6-151::LEU2/rec6-151::LEU2 leu1-32/leu1-32 ade6-M210/ade6-M216*
ED2	*h⁺/h⁻ rec8::ura4⁺/rec8::ura4⁺ ura4-D18/ura4-D18 rec11-156::LEU2/rec11-156::LEU2 leu1-32/leu1-32 ade6-M210/ade6-M216*
ED3	*h⁺/h⁻ rec10-155::LEU2/rec10-155::LEU2 leu1-32/leu1-32 ade6-M210/ade6-M216*
ED4	*h⁺/h⁻ rec11-156::LEU2/rec11-156::LEU2 leu1-32/leu1-32 ade6-M210/ade6-M216*
ED5	*h⁺/h⁻ rec12-152::LEU2/rec12-152::LEU2 leu1-32/leu1-32 ade6-M210/ade6-M216*
ED6	*h⁺/h⁻ rec14-161::LEU2/rec14-161::LEU2 leu1-32/leu1-32 ade6-M210/ade6-M216*
ED7	*h⁺/h⁻ rec15::kanMX/rec15::kanMX ade6-M210/ade6-M216*
ED8	*h⁺/h⁻ meu13::ura4⁺/meu13::ura4⁺ ura4-D18/ura4-D18 leu1-32/leu1-32 his2/+ ade6-M210/ade6-M216*
ED9	*h⁺/h⁻ rep1::ura4⁺/rep1::ura4⁺ ura4-D18/ura4-D18 ade6-M210/ade6-M216*
L 975	*h⁺*
AY261-1C	*h⁻ leu1 lys1 cen2(D107)::kan^r-ura^4-lacOp his7⁺::lacI-GFP*
67	*h⁺ rec10-155::LEU2 leu1-32 ade6-M216*
95	*h⁻ rec10-155::LEU2 leu1 cen2(D107)::kan^r-ura^4-lacOp his7⁺::lacI-GFP*
68-2710	*h⁺ rec8::ura4⁺ ura4-D18 lys1-131*
101	*h⁻ rec8::ura4⁺ leu1 lys1 ura4 cen2(D107)::kan^r-ura^4-lacOp his7⁺::lacI-GFP*
70	*h⁺ rec11-156::LEU2 leu1-32 ade6-M216*
100	*h⁻ rec11-156::LEU2 leu1 ade6-M216 cen2(D107)::kan^r-ura^4-lacOp his7⁺::lacI-GFP*
CT2111-2	*h^{90} leu1 lys1 ura4 ade6-M216 cen2(D107)::kan^r-ura^4-lacOp his7⁺::lacI-GFP*
119	*h^{90} rec10-155::LEU2 leu1 ura4 ade6-M216 cen2(D107)::kan^r-ura^4-lacOp his7⁺::lacI-GFP*
161	*h^{90} rec8::ura4⁺ leu1 lys1 ura4 ade6-149 cen2(D107)::kan^r-ura^4-lacOp his7⁺::lacI-GFP*
121	*h^{90} rec11-156::LEU2 leu1 ura4 ade6-M210 cen2(D107)::kan^r-ura^4-lacOp his7⁺::lacI-GFP*
153	*h⁻ leu1 lys1 ura4 ade6-M216 his2[::kan^r-ura^4-lacOp] his7⁺::lacI-GFP*
156	*h⁻ rec10-155::LEU2 leu1 ura4 ade6-M216 his2[::kan^r-ura^4-lacOp] his7⁺::lacI-GFP*
157	*h⁻ rec8::ura4⁺ leu1 lys1 ura4 his2[::kan^r-ura^4-lacOp] his7⁺::lacI-GFP*
155	*h⁻ rec11-156::LEU2 leu1 ura4 ade6-M216 his2[::kan^r-ura^4-lacOp] his7⁺::lacI-GFP*
105	*h⁻ ura4-D18 leu1-32*
AY234-6B	*h⁺ leu1 lys1 ura4 ade6-M216 ade1[::kan^r-ura^4-lacOp] his7⁺::lacI-GFP*
68	*h⁻ rec10-155::LEU2 leu1-32 ade6-M210*
116	*h⁺ rec10-155::LEU2 leu1 lys1 ura4 ade6-M216 ade1[::kan^r-ura^4-lacOp] his7⁺::lacI-GFP*
128	*h⁻ rec8::ura4⁺ ura4-D18 leu1-32 ade6-149*
143	*h⁺ rec8::ura4⁺ leu1 ura4 ade6 ade1[::kan^r-ura^4-lacOp] his7⁺::lacI-GFP*
132	*h⁻ rec11-156::LEU2 leu1-32 lys1 ade6-M210*
117	*h⁺ rec11-156::LEU2 leu1 lys1 ade6 ade1[::kan^r-ura^4-lacOp] his7⁺::lacI-GFP*
AY208-21A	*h⁻ leu1 lys1 ura4 ade8[::kan^r-ura^4-lacOp] his7⁺::lacI-GFP*
143	*h⁻ rec10-155::LEU2 leu1 ura4 ade6-M216 ade8[::kan^r-ura^4-lacOp] his7⁺::lacI-GFP*
142	*h⁻ rec8::ura4⁺ leu1 lys1 ura4 ade8[::kan^r-ura^4-lacOp] his7⁺::lacI-GFP*
146	*h⁻ rec11-156::LEU2 leu1 ade6-M216 ade8[::kan^r-ura^4-lacOp] his7⁺::lacI-GFP*
JW555	*h^{90} leu1-32 lys1 ura4-D18 ade6-M216 his2[::kan^r-ura^4-lacOp] his7⁺::lacI-GFP*
148	*h^{90} rec10-155::LEU2 leu1 ura4-D18 ade6-M216 his2[::kan^r-ura^4-lacOp] his7⁺::lacI-GFP*
JW558	*h^{90} leu1 lys1 ura4-D18 ade6-M216 ade1[::kan^r-ura^4-lacOp] his7⁺::lacI-GFP*
149	*h^{90} rec10-155::LEU2 leu1 lys1 ade6 ura4-D18 ade1[::kan^r-ura^4-lacOp] his7⁺::lacI-GFP*
159	*h^{90} leu1 ura4 ade8[::kan^r-ura^4-lacOp] his7⁺::lacI-GFP*
166	*h^{90} rec10-155::LEU2 leu1 ade8[::kan^r-ura^4-lacOp] his7⁺::lacI-GFP*

decreased homologous pairing for the first time (Molnar et al., 1995). However, *rec8* turned out to be a meiotic cohesin (Parisi et al., 1999; Watanabe and Nurse, 1999). As a consequence, direct evidence for the involvement of linear elements in meiotic chromosome functions is still lacking.

Our preliminary observations have shown that linear elements are altered or impaired in several meiotic recombination-deficient mutants, indicating a connection between linear element formation, recombination, and perhaps other meiotic chromosome functions. To learn more about the functions of linear elements we studied linear element formation in those *rec* mutants that show a strong (*rec6, rec12, rec14, rec15, rec16*) or intermediate (*rec10, rec11*) decrease in meiotic recombination (Ponticelli and Smith, 1989; DeVeaux et al., 1992). Because of its important role in meiotic chromosome pairing, *meu13*, homolog of *HOP2* in *S. cerevisiae* (Nabeshima et al., 2001), was also investigated. In this study we describe several mutants with altered linear element morphology, and discuss the possible reasons for the morphological changes. This investigation of linear element formation has provided a structural explanation for the region-specificity of loss of recombination observed in the *rec8, rec10* and *rec11* mutants. We show that linear elements are dispensable for sister chromatid cohesion, but contribute to full level homologous pairing of chromosome arms.

Materials and Methods

Strains, media and standard genetic methods

S. pombe strains used in this study are listed in Table 1. The *rec15::kanMX* mutant was created according to the method of Bähler et al. (Bähler et al., 1998). In this construct the whole ORF of *rec15* was replaced by the *kanMX6* module. Other deletions/disruptions used in this study were described previously: [*rec8::ura4⁺* (Parisi et al., 1999); *rec6-151::LEU2* and *rec12-152::LEU2* (Lin and Smith, 1994); *rec10-155::LEU2* (Lin and Smith, 1995); *rec11-156::LEU2* (Li et al., 1997); *rec14-161::LEU2* (Evans et al., 1997); *meu13::ura4⁺* (Nabeshima et al., 2001); and *rep1::ura4⁺*. *rep1* (Sugiyama et al., 1994) is identical to *rec16* (Ding and Smith, 1998). To visualize different chromosomal regions, the lacI/lacO system was used. Strains designated *his7⁺::lacI-GFP* have GFP-tagged lacI inserted at the *his7*

locus (Nabeshima et al., 1998). The lacO tandem repeats, together with the *ura4*$^+$ and *kan*^{r} genes, were integrated at chromosomal loci indicated in Fig. 7F.

YEA (yeast extract agar) and YEL (yeast extract liquid) complete media, and MEA (malt extract agar) sporulation medium were as described previously (Gutz et al., 1974). Diploid strains JB6 and ED1 to ED9 (Table 1) were constructed through interrupted mating (Gutz et al., 1974). Diploid colonies are prototrophic and white on YEA medium as a result of interallelic complementation between the *ade6-M216* and *ade6-M210* mutations (Moreno et al., 1991). PM (*S. pombe* minimal) and PM-N (PM without NH_4Cl) media used for meiotic time-courses were as described (Beach et al., 1985; Watanabe et al., 1988). Induction of mating and meiosis was done on MEA plates, and living cells were observed microscopically in EMM2-N liquid medium [EMM2 minimal medium without nitrogen source (Moreno et al., 1991)].

Time-course experiments

Meiotic cultures of diploid strains were prepared as described (Bähler et al., 1993). Shifting a culture to meiotic conditions at highly different cell titers changes the overall progression of the meiotic time-course [e.g. compare Fig. 5B and Fig. 5C in Molnar et al. (Molnar et al., 1995)]. Therefore, in order to compare the different mutants, care was taken to grow each culture to a cell titer of 1×10^7 to 2×10^7 in PM medium, before meiosis was induced in PM-N. Samples were taken hourly for DAPI staining of nuclei (Bähler et al., 1993) and for spreading. Nuclear spreads were prepared and silver-stained as described (Bähler et al., 1993), with one modification. To digest the cell walls 1 mg/ml lysing enzyme L2265 (Sigma) was used instead of Novozyme 234. Silver-stained nuclei were examined with a Philips EM300 at 60 kV (Philips Eindhoven, The Netherlands). Approximately 100 silver-stained and 200 DAPI-stained nuclei were evaluated at each time point. At least two independent time courses were carried out with each mutant.

Examination of sister chromatid cohesion, chromosome segregation and homologous pairing

Sister chromatid cohesion, chromosome segregation and pairing of homologous chromosomes were monitored in living fission yeast cells carrying the lacI/lacO system. Mating and meiosis were induced by transferring homothallic (h^{90}) or crossing heterothallic (h^+ and h^-) strains on MEA and incubating the plates overnight at 26°C. Hoechst 33342, a DNA-specific fluorescence dye, was used to identify the different meiotic stages in living cells. Cells were stained with 5 μg/ml Hoechst 33342 in distilled water for 15 minutes at room temperature, resuspended in EMM2-N, and mounted on a coverslip for microscopic examination. Specimens were observed at 26°C on the CCD microscope system described previously (Molnar et al., 2001a). In order to monitor the position and number of GFP signals, images were taken with an exposure time of 0.5 seconds, in 10 optical sections covering the whole nucleus. Images were analyzed after deconvolution using the Delta Vision program (Applied Precision, Seattle, WA).

Results

Linear element formation in meiotic recombination-deficient mutants

To study the phenotype of linear elements in meiotic recombination-deficient mutants meiotic time-course experiments were carried out with strains ED1 to ED9, and with JB6 as a control (Table 1). Fig. 1 shows the four regular morphological classes of linear elements (Fig. 1A-D), the quantitation of the different classes (Fig. 1E) and the timing of meiotic events followed by DAPI staining (Fig. 1F) in a time-course of the JB6 strain. A control time-course can be described briefly as follows. First, nuclei with a few, short elements can be detected (class I, Fig. 1A). Later the elements seem to contact each other and become entangled (class IIa, network; Fig. 1B), or in other nuclei several elements align closely (class IIb, bundle; Fig. 1C). Then nuclei with single, long elements appear (class III, Fig. 1D). The degradation of elements occurs through class I morphology. [For a more detailed description of a standard meiotic time course, see Bähler et al. (Bähler et al., 1993).]

A comparison of the morphology of elements and the frequency of their classes in the different meiotic recombination-deficient mutants with the control revealed that the mutants fall into four groups. (1) Some recombination-deficient mutants showed regular phenotype qualitatively (morphology of elements) and quantitatively (frequency of classes). *rec6*, *rec15*, and the previously investigated *rec7* mutant (Molnar et al., 2001b) belong to this group (data not shown). (2) In the *rec12*, *rec14* and *meu13* mutants both the morphology and frequency of certain classes were altered, but the observed morphologies still resembled wild-type. (3) *rec11* showed strongly impaired linear element morphology that had been observed before with the other cohesin mutant *rec8* (Molnar et al., 1995). (4) In the *rec10* and *rec16/rep1* mutants no traces of linear elements were found.

Mutants with altered linear element formation

To investigate the phenotype of linear elements in the *rec12* mutant meiotic time courses of strain ED5 (Table 1) were analyzed. In this mutant two of the observed morphologies of linear elements: class I (short elements, Fig. 2A) and class IIa (network, Fig. 2B) strongly resembled those seen in the control strain. However, class IIb and class III looked different. Instead of having a single, long bundle (Fig. 1C), class IIb nuclei contained several, shorter pieces of bundles (Fig. 2C). The class III nuclei of *rec12* can be characterized by an abundance of single long elements, some of which were unusually long (Fig. 2D). The most striking feature of the *rec12* mutant was the high frequency of class III nuclei throughout the whole time-course (Fig. 2E). A statistical analysis of the time course (5×2 table test) clearly indicated that the distribution of different classes of linear elements in the *rec12* mutant is significantly different from that of the wild-type ($P<0.005$). Class III was the most frequently observed phenotype in statistical sense as well, while class I was rare in the *rec12* mutant. This suggests that short elements (class I) elongated quickly at the beginning of the time course, and their disassembling at late phases was also quicker in this mutant than in the wild-type. Meiotic divisions occurred early in this mutant (Fig. 2F), and the intensive sporulation prevented the preparation and evaluation of spreads at later than 8 hour time points.

In the *rec14* mutant (strain ED6, Table 1) linear element formation began with regular class I morphology (Fig. 3A), but nuclei of this type remained scarce throughout prophase (Fig. 3E). The single short elements developed into networks (class IIa, Fig. 3B), which is the most frequently seen morphology in *rec14* (Fig. 3E). Many of these networks contained loosely connected elements and showed a sort of ‘moth-eaten’

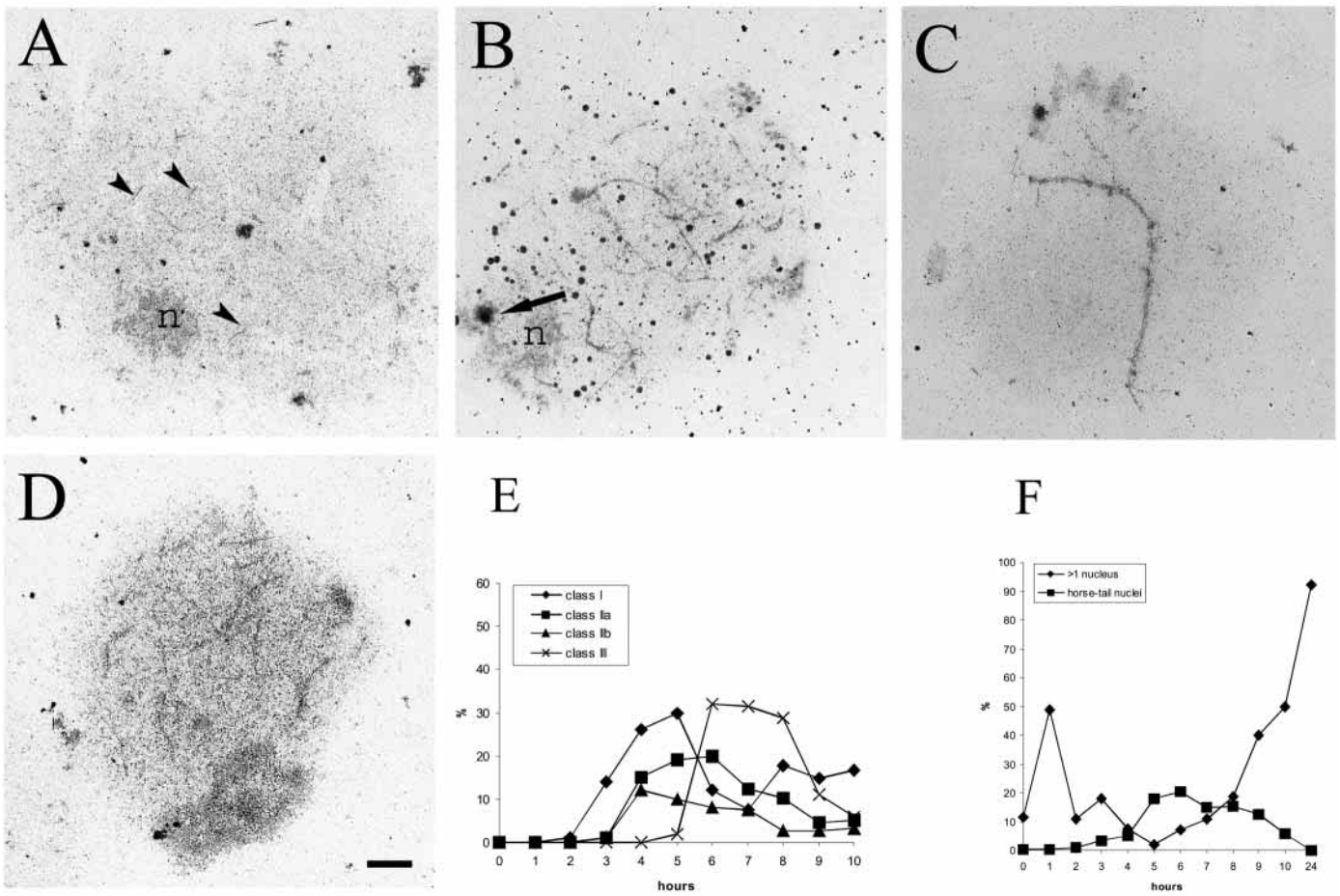

Fig. 1. Linear element morphologies and temporal comparison of cytological events in a time-course of the JB6 control strain. (A-D) Electron micrographs of spread and silver-stained nuclei of different linear element morphologies. (A) Single, short elements in a class I nucleus. Arrowheads indicate linear elements; 'n' is the nucleolus. (B) Developing network in a class IIa nucleus. The arrow points at the spindle pole body (SPB), which is located close to the nucleolus (n). (C) Bundle in a class IIb nucleus. (D) Single, long elements in a class III nucleus. Bar, 1 μm. (E) Quantitation and temporal order of the different morphological classes. (F) Timing of cytological events as followed by DAPI staining. Horse-tail nuclei indicate meiotic prophase. Cells with more than one nucleus have progressed through the first meiotic division. After meiotic induction cells undergo a final mitotic division (peak at 1 hour) before they enter meiosis from G1 phase.

appearance (Fig. 3B, right). These nuclei may represent impaired network morphology. Alternatively, since the high frequency of networks suggests that *rec14* nuclei spend longer time at this stage, the moth-eaten morphology may represent processing or disassembly of networks. Class IIb nuclei were rare, and contained 2-4 short pieces of bundles (Fig. 3C). The processing of linear elements seems to pass through the single long element stage (class III, Fig. 3D), but the quick progression to meiosis I and the heavy sporulation prevented an evaluation of the latest stages (Fig. 3E,F). The difference in the distribution of linear element classes between the *rec14* and wild-type strains is statistically significant ($P<0.005$). Classes I and IIa show the major differences.

Time-course experiments with strain ED8 (Table 1) revealed that linear element formation begins in an unusual way in the *meu13* mutant. Instead of class I, small, compact nuclei with 1-2 pieces of bundle-like structures started the process (class IIb early, Fig. 4A). These nuclei were distinguishable from those appearing later (class IIb late, Fig. 4C) by their smaller size. Because the same specimens contained nuclei of different sizes and linear element morphologies (Fig. 4E, see time points 5 to 7 hours), these compact nuclei are not likely to be spreading artifacts. Nuclei designated class IIb late (Fig. 4C) were larger and contained 2 to 4 short bundle pieces. Networks (class IIa) were also altered in the *meu13* mutant. They frequently appeared as a kind of combination of the network and regular bundle morphologies (Fig. 4B). Single long elements was the morphology observed latest (Fig. 4D). Divisions in *meu13* occurred with a timing similar to the control (Fig. 4F). Because the *meu13* mutant showed some obvious differences in LE organization compared to the wild-type (lack of class I nuclei and two types of bundles), we did not carry out a statistical analysis on the distribution of different LE classes. The same applies for the cohesin mutants (see below).

Linear elements in cohesin mutants

Experiments with strain ED4 (Table 1) revealed that the morphologies of linear elements in the *rec11* mutant are

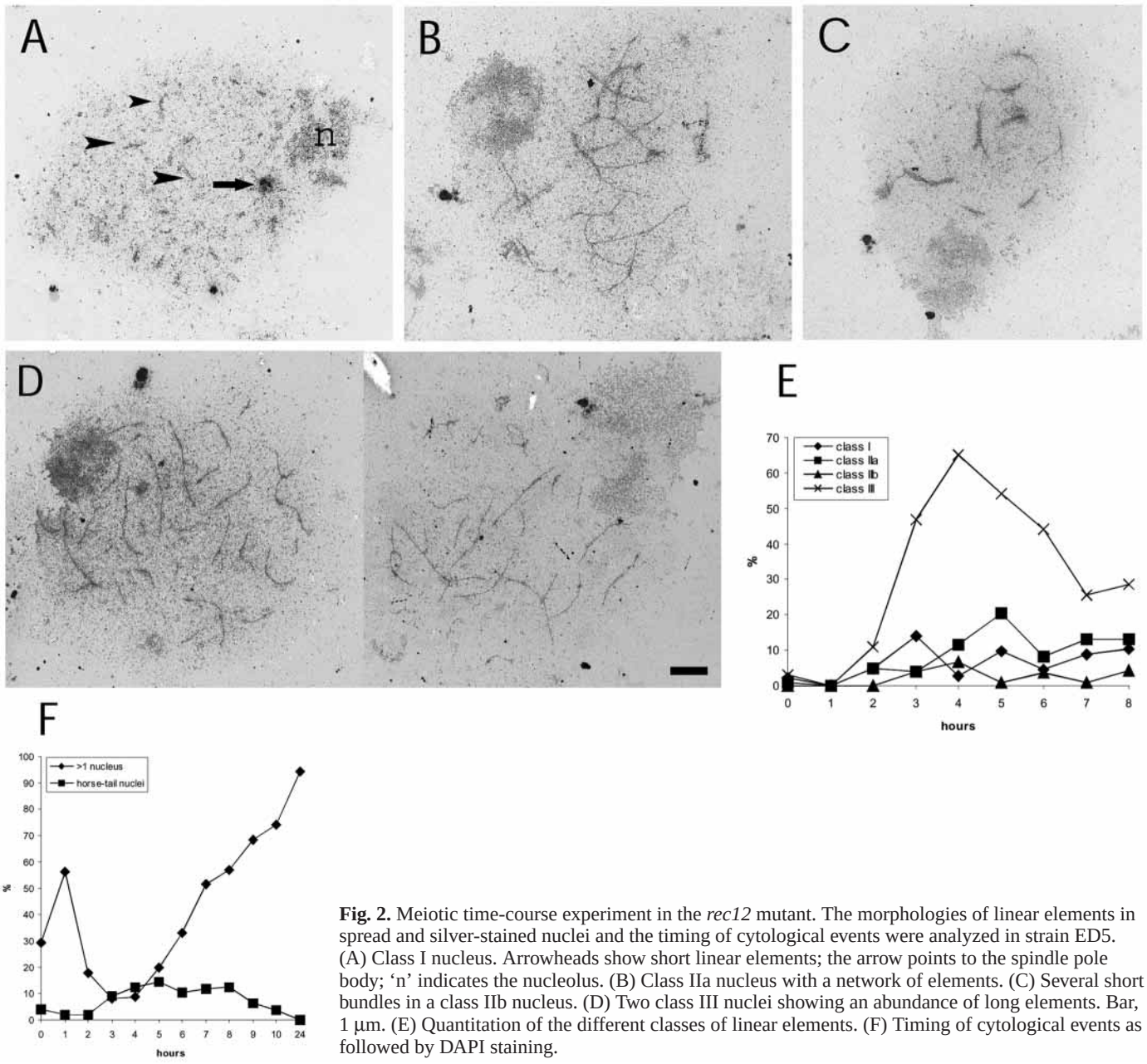

Fig. 2. Meiotic time-course experiment in the *rec12* mutant. The morphologies of linear elements in spread and silver-stained nuclei and the timing of cytological events were analyzed in strain ED5. (A) Class I nucleus. Arrowheads show short linear elements; the arrow points to the spindle pole body; 'n' indicates the nucleolus. (B) Class IIa nucleus with a network of elements. (C) Several short bundles in a class IIb nucleus. (D) Two class III nuclei showing an abundance of long elements. Bar, 1 μm. (E) Quantitation of the different classes of linear elements. (F) Timing of cytological events as followed by DAPI staining.

virtually indistinguishable from those seen in *rec8*. Therefore, the same designation of classes was used to describe *rec11* as that previously used for the *rec8-110* mutant (Molnar et al., 1995). Class A stands for nuclei with a few, very short elements (Fig. 5A). In class B nuclei usually 2 or 3 short and thick elements were visible (Fig. 5B). Class C nuclei appeared last, and contained a single long element (Fig. 5C,D). The above morphologies suggest a severe defect in linear element formation. It is a distinct phenotype, observed so far only in the meiotic cohesin mutants *rec8* and *rec11* [(Molnar et al., 1995) and this study]. Thus we call it the cohesion-defect phenotype of linear elements. The same morphologies were detected in strain ED2 (Table 1) where both meiotic cohesins are deleted (compare the nuclei in Fig. 5B and C, and data not shown).

Mutants that do not form linear elements

Two of the meiotic recombination-deficient mutants, *rec16/rep1* and *rec10*, did not contain any element-like structures. The majority of cells in the *rec16/rep1* strain ED9 (Table 1) did not undergo meiosis. In two time-course experiments, 18% and 25% final sporulation was measured. Although only a small fraction of cells underwent meiosis, nuclei in meiotic prophase were still detectable in the electron microscope. Before meiotic prophase, the spindle pole body (SPB) locates far from the nucleolus, and consists of a single body or two bodies of equal sizes (Bähler et al., 1993). Normally, meiotic prophase nuclei contain linear elements and have their spindle pole body (SPB) located close to the nucleolus. The SPB consists of a large and two adjacent smaller bodies in meiotic prophase [see Figs 1-5 (Bähler et al.,

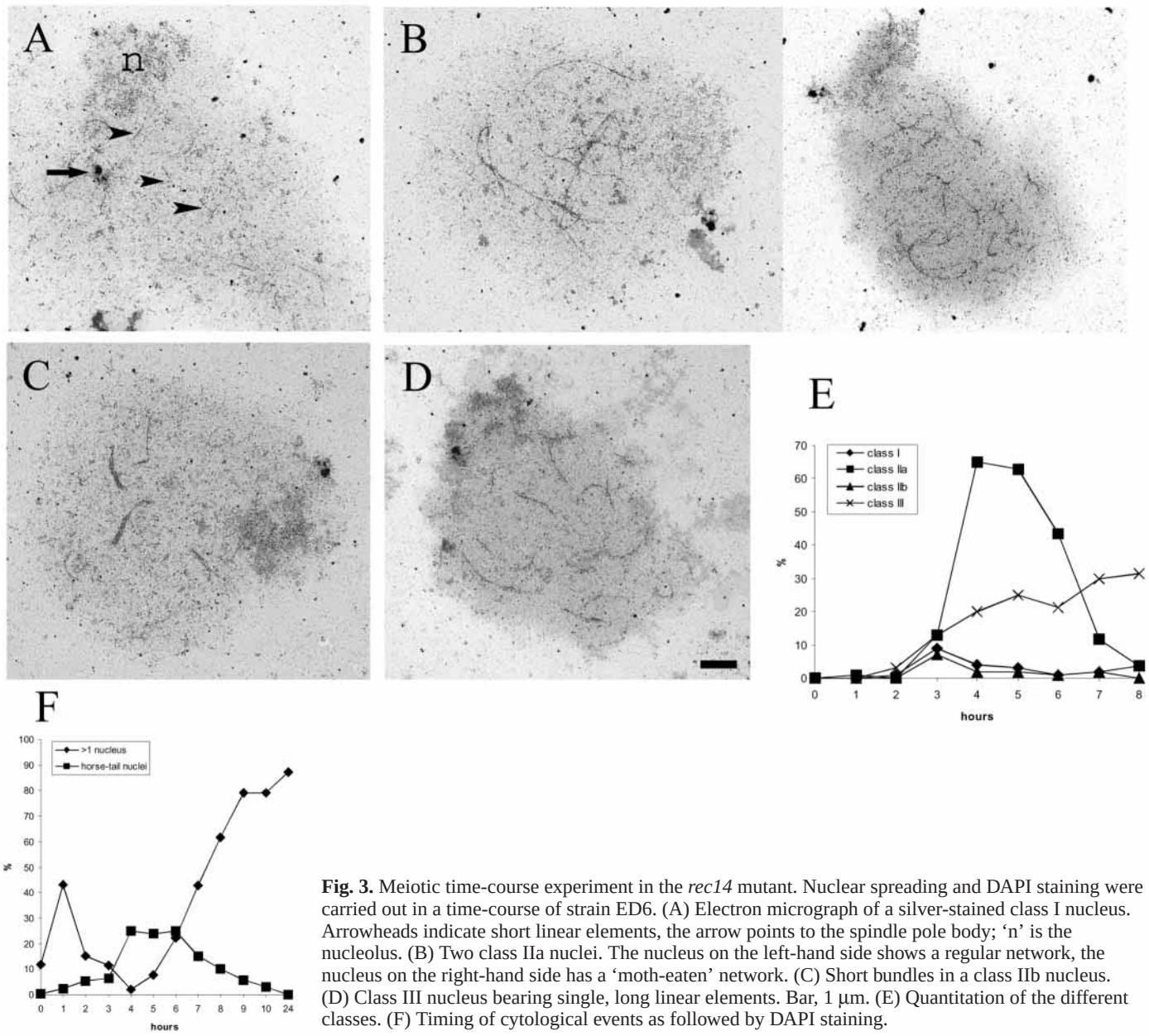

Fig. 3. Meiotic time-course experiment in the *rec14* mutant. Nuclear spreading and DAPI staining were carried out in a time-course of strain ED6. (A) Electron micrograph of a silver-stained class I nucleus. Arrowheads indicate short linear elements, the arrow points to the spindle pole body; 'n' is the nucleolus. (B) Two class IIa nuclei. The nucleus on the left-hand side shows a regular network, the nucleus on the right-hand side has a 'moth-eaten' network. (C) Short bundles in a class IIb nucleus. (D) Class III nucleus bearing single, long linear elements. Bar, 1 μm. (E) Quantitation of the different classes. (F) Timing of cytological events as followed by DAPI staining.

1993)]. At time points 3 to 9 hours, up to 20% of nuclei showed this morphology in the *rec16* mutant, but these meiotic nuclei never contained linear elements (Fig. 6A). Sugiyama et al. have shown that *rec16/rep1* is deficient in premeiotic DNA synthesis (Sugiyama et al., 1994). This explains the described severe defects.

Meiotic time-courses with strain ED3 (Table 1) gave an unexpected result. In the *rec10* mutant no trace of linear elements could be observed. The *rec10* mutant progressed through meiosis similarly to the JB6 control strain (Fig. 6B). In *rec10*, empty nuclei with meiotic prophase SPB configuration were observed with a frequency similar to that seen in linear-element-containing nuclei in the control. Horse-tail nuclei appeared with similar dynamics in the two strains. In contrast to *rec16/rep1*, the *rec10* mutant underwent meiosis efficiently (Fig. 6B). Thus *rec10* can be a useful tool to evaluate the consequences of the lack of linear elements in fission yeast.

Regular sister chromatid cohesion in *rec10*

It has been proposed that linear elements have a role in meiotic chromatin organization and that they may be necessary for the proper completion of meiotic chromosome functions (Bähler et al., 1993). In order to test the involvement of linear elements in sister chromatid cohesion, *rec10* and control heterothallic strains bearing the lacI-GFP/lacO recognition system were crossed with strains lacking GFP labeling (heterozygous cross for GFP). Deletion strains of the meiotic cohesins *rec8* and *rec11* (Table 1) were also investigated. Sister chromatid cohesion was checked at the centromere and three different loci along the right arm of chromosome II (Fig. 7F). Cells in meiotic prophase (horse-tail nuclei) were identified after Hoechst 33342 staining, and the number of GFP signals was determined in living cells (see Materials and Methods). In a heterozygous cross a single GFP signal indicates regular sister chromatid cohesion. Appearance of two separated GFP signals

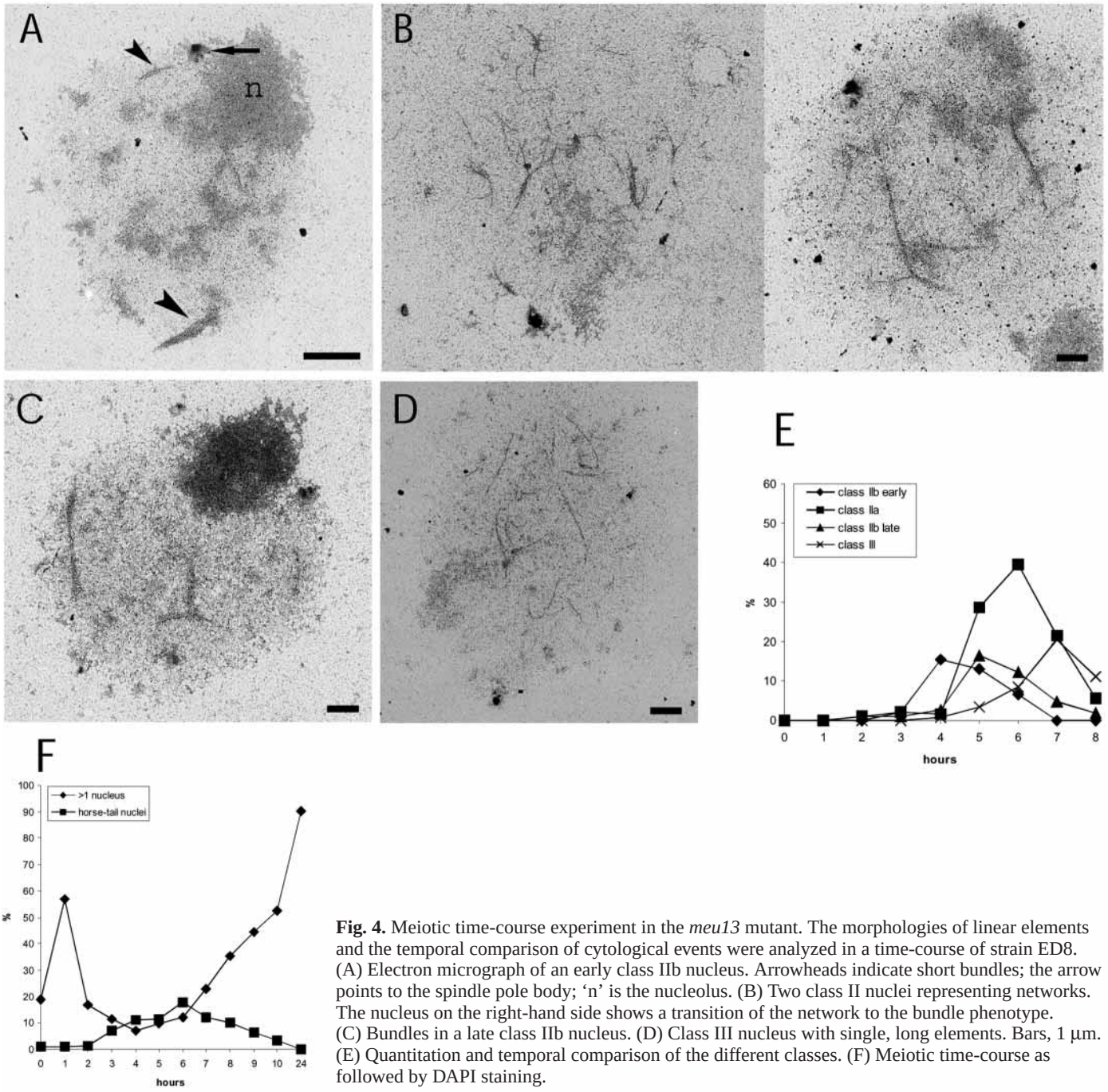

Fig. 4. Meiotic time-course experiment in the *meu13* mutant. The morphologies of linear elements and the temporal comparison of cytological events were analyzed in a time-course of strain ED8. (A) Electron micrograph of an early class IIb nucleus. Arrowheads indicate short bundles; the arrow points to the spindle pole body; 'n' is the nucleolus. (B) Two class II nuclei representing networks. The nucleus on the right-hand side shows a transition of the network to the bundle phenotype. (C) Bundles in a late class IIb nucleus. (D) Class III nucleus with single, long elements. Bars, 1 μm. (E) Quantitation and temporal comparison of the different classes. (F) Meiotic time-course as followed by DAPI staining.

is an obvious sign of the loss of sister chromatid cohesion. Sometimes nuclei with two closely associated but still unseparated signals were detected. Because it was frequently seen in the cohesin mutants, this doubling of the GFP signal probably indicates a loosening of sister chromatid association. Nuclei with separated and doubled GFP signals were scored separately (Fig. 7).

Sister chromatids were rarely separated at the centromere in prophase in the *rec8* and *rec11* mutants (Fig. 7A). In contrast, an increased impairment of sister chromatid cohesion was detected along the chromosome arm in both mutants (Fig. 7B-D). The degree of impairment was fairly constant at all loci examined in *rec8*. In *rec11*, a slight increase was observed towards the telomere. This is in contrast to the *rec10* mutant where only slight aberrancies were detected at each locus (Fig. 7A-D).

χ^2 test showed no statistical difference in sister chromatid cohesion between the wild-type and the *rec10* mutant at any of the chromosomal loci. A comparison of *rec8* and *rec11* showed that there clearly was no difference between them either. To get an idea about the difference between the wild-type and the cohesin mutants, we compared the combined data of the wild-type strains (wt and *rec10*) to the combined data of the cohesin mutant strains (*rec8* and *rec11*). The reduction in sister

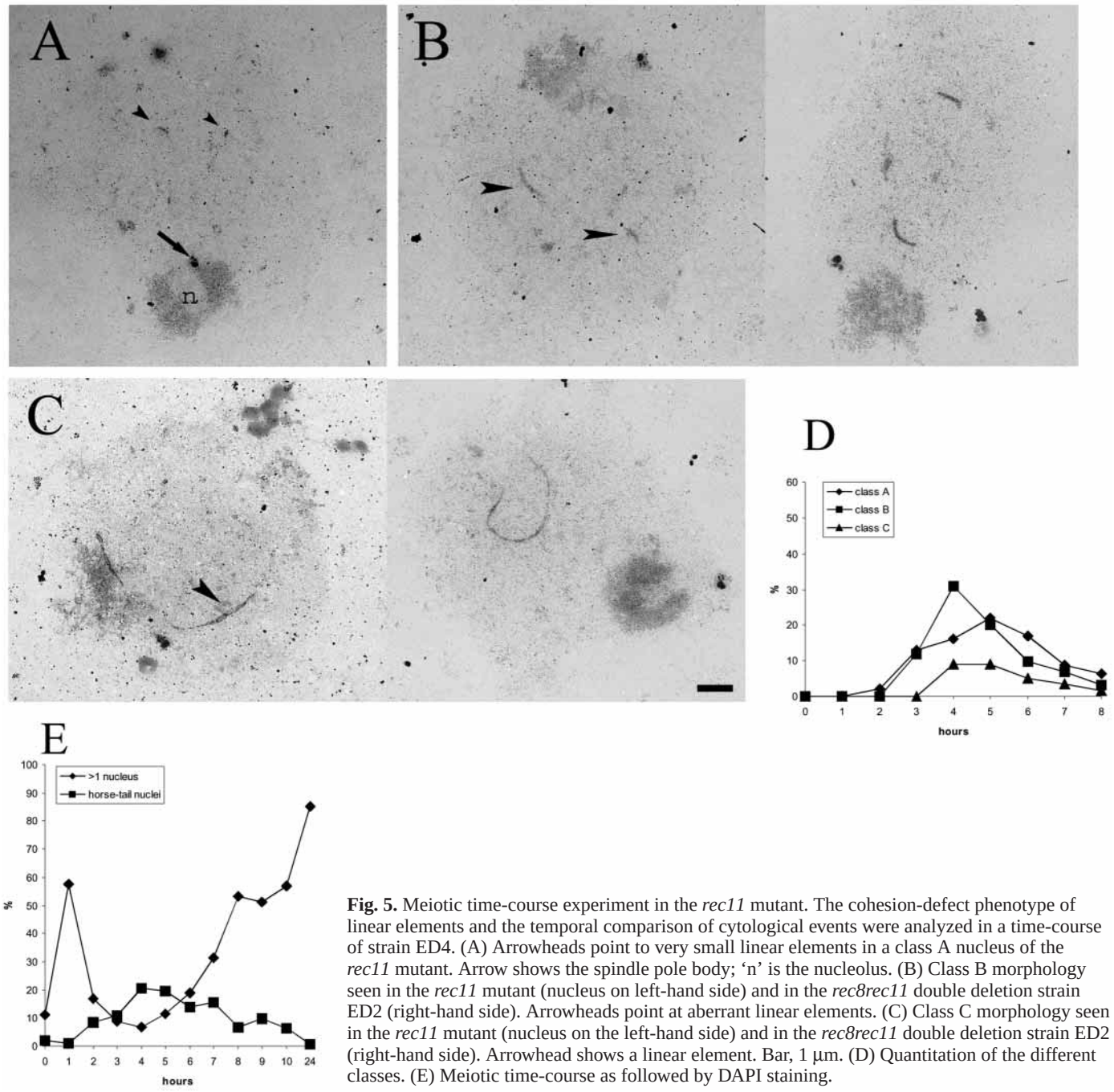

Fig. 5. Meiotic time-course experiment in the *rec11* mutant. The cohesion-defect phenotype of linear elements and the temporal comparison of cytological events were analyzed in a time-course of strain ED4. (A) Arrowheads point to very small linear elements in a class A nucleus of the *rec11* mutant. Arrow shows the spindle pole body; 'n' is the nucleolus. (B) Class B morphology seen in the *rec11* mutant (nucleus on left-hand side) and in the *rec8rec11* double deletion strain ED2 (right-hand side). Arrowheads point at aberrant linear elements. (C) Class C morphology seen in the *rec11* mutant (nucleus on the left-hand side) and in the *rec8rec11* double deletion strain ED2 (right-hand side). Arrowhead shows a linear element. Bar, 1 μm. (D) Quantitation of the different classes. (E) Meiotic time-course as followed by DAPI staining.

chromatid cohesion in the cohesin mutants was statistically not significant at the centromere ($0.05<P<0.1$). In contrast, cohesion is significantly reduced at all the other loci (*his2*, *ade1*, *ade8*) examined in the cohesin mutants ($P=0.005$). We conclude that the cohesion of sister chromatids is basically intact despite the lack of linear elements in meiotic prophase of *rec10*.

Precocious separation of sister chromatids may occur at the first meiotic division. It is conceivable that cytologically invisible pieces of linear elements remain at the chiasmata and support the proper segregation at meiosis I. Therefore, we examined chromosome segregation at the first meiotic division in each mutant. Cells having two nuclei were identified after Hoechst 33342 staining and the number of GFP signals was determined. When both nuclei carried a GFP signal in a heterozygous cross, sister chromatids segregated prematurely. To examine segregation of homologous chromosomes, homothallic strains (homozygous cross for GFP, Table 1) were also analyzed. In a homozygous cross both homologous chromosomes have GFP labeling. If one of the sister nuclei after meiosis I had no GFP signal, nondisjunction of homologous chromosomes had occurred. In accordance with previous studies (Watanabe and Nurse, 1999; Molnar et al., 2001a), a high level of precocious sister chromatid separation was detected in *rec8* (PSSC; Fig. 7E). Precocious sister chromatid separation was rare in *rec10* and *rec11*, but both

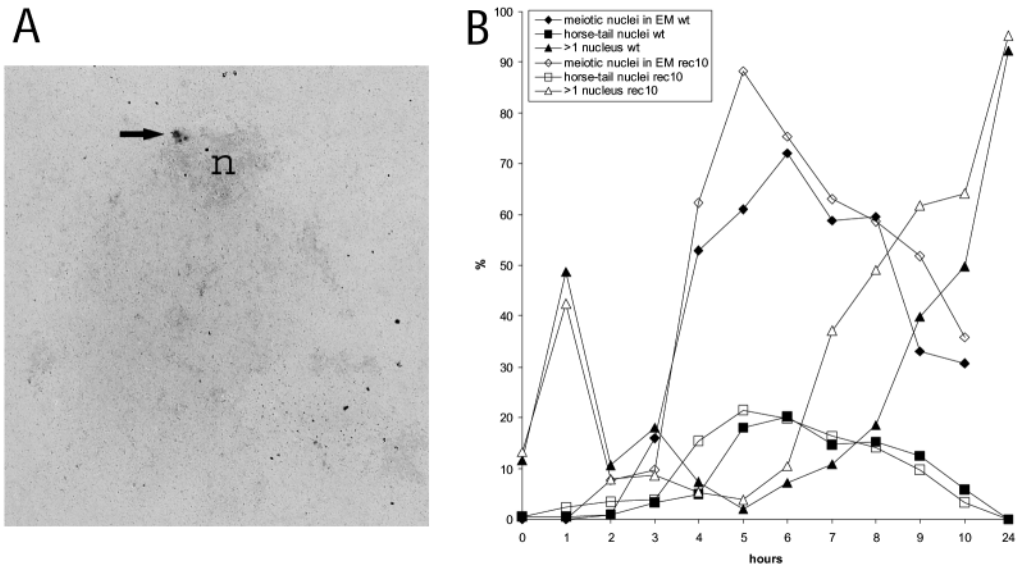

Fig. 6. Meiotic time-course experiment in the *rec10* mutant. (A) Empty meiotic nucleus. The chromatin region is faintly stained by silver nitrate; 'n' indicates the more densely stained nucleolus. The arrow points to the spindle pole body which consists of a large and two small bodies. (B) A comparison of the timing of cytological events in the *rec10* mutant ED3 and the control JB6 strain. Meiotic nuclei were identified in the electron microscope after spreading and silver staining. The horse-tail stage and the progression of meiotic divisions were analyzed in DAPI-stained cells.

Table 2. Homologous chromosome pairing

	cen2 locus		*his2* locus		*ade1* locus		*ade8* locus	
	Pairing (%)	N*	Pairing (%)	N*	Pairing (%)	N*	Pairing (%)	N*
rec$^+$	40	220	24.5	220	31.4	204	35.5	220
rec10	39.6	202	20.9	220	21.4	220	30.9	220

*Number of horse-tail nuclei examined.

mutants showed high level of chromosomal nondisjunction at the first division (NDJI; Fig. 7E). A comparison of the combined data of the *rec10* and *rec11* strains to the combined data of the wt and *rec10* strains showed a statistically highly significant difference in NDJI (P=0.005). In summary, our observations with GFP-labeled chromosomes in living cells suggest that linear elements are dispensable for sister chromatid cohesion in fission yeast.

Homologous chromosome pairing is decreased in *rec10* in a region-specific manner

Next we asked whether linear elements are necessary for homologous chromosome pairing. Homothallic *rec10* (strains 119, 148, 149 and 166) and control (CT2111-2, JW555, JW558 and 159) strains (Table 1) bearing GFP labeling at different chromosomal loci (Fig. 7F) were examined. Horse-tail stage cells were identified after Hoechst 33342 staining and the GFP signals were analyzed as described in Materials and Methods. Homologous chromosomes were scored as paired when their GFP signals touched each other or only a single signal was visible. The results are summarized in Table 2.

The highest level of chromosome 'pairing' was measured at the centromere in the control strain. [Actually, in fission yeast a clustering of all the centromeres occurs in prophase (Scherthan et al., 1994).] Along the chromosome arm, an increase of pairing was detectable towards the telomere. The *rec10* mutant showed wild-type level of clustering of centromeres but decreased pairing at all other loci examined. A comparison of the homologous pairing in *rec10* to the control (Fig. 8) revealed that in *rec10* the impairment was slight (statistically not significant) at the *his2* and *ade8* loci. These loci are located towards the centromere and telomere ends of the chromosome arm, respectively (Fig. 7F). At the *ade1* locus, which is situated in the middle of the right arm of chromosome II, significantly decreased pairing ($0.01<P<0.025$) was detected. These results suggest that linear elements contribute to regular homologous chromosome pairing and their role is especially important in the interstitial regions of chromosome arms.

Discussion

A distinguishing feature of meiosis is the appearance of proteinaceous structures that connect homologous chromosomes. In most of the examined eukaryotes synaptonemal complexes (SC) develop during the first meiotic prophase. The functions of this complicated structure are not really understood (Zickler and Kleckner, 1999; Roeder, 1997; Kleckner, 1996). Fission yeast is an exception. It does not form SC but instead linear elements, which have been proposed to be minimal structures required for proper chromosome functions during meiotic prophase and at the first meiotic division (Bähler et al., 1993; Kohli, 1994; Kohli and Bähler, 1994; Scherthan et al., 1994). The elaboration of the function(s) of linear elements may contribute to a better understanding of the mechanism of meiosis and may help to understand the functions of the synaptonemal complex as well.

Conclusions from the analysis of mutants with altered linear element formation and processing

Three of the recombination deficient mutants, *rec12*, *rec14* and *meu13* showed altered linear element formation, but the morphology patterns were close to those seen in wild-type. Because the prophase stages in other organisms are defined by the development of the synaptonemal complex, a similar subdivision of meiotic prophase in fission yeast is not possible. A correlation of recombination events other than DSBs, as detected by physical analysis, with the cytological changes is still missing in fission yeast. Nevertheless, it is noteworthy that the three mutations caused different changes of morphologies and their frequencies, at different stages of meiotic prophase. This argues for a biological significance of the different linear element morphologies.

Rec12 is a homolog of Spo11, a protein that forms recombination-initiating double-strand breaks in *S. cerevisiae* (Cervantes et al., 2000; Davis and Smith, 2001; Keeney et al., 1997). The conservation of the catalytic site suggests an identical function in *S. pombe* (Keeney et al., 1997; Cervantes et al., 2000). In the *rec12* mutant of fission yeast no detectable meiosis-specific breakage of chromosomes occurs (Cervantes et al., 2000; Young et al., 2002). Therefore, the *rec12* mutant is an appropriate tool to address a possible interdependence of formation of double-strand breaks and linear elements. Linear elements, although with altered morphology, were observed in the *rec12* mutant (Fig. 2). Consequently, the formation of linear elements is not dependent on the occurrence of double-strand breaks. Analysis of the *rec6*, *rec7* (Molnar et al., 2001b) and *rec15* mutants confirmed this conclusion. They are defective in

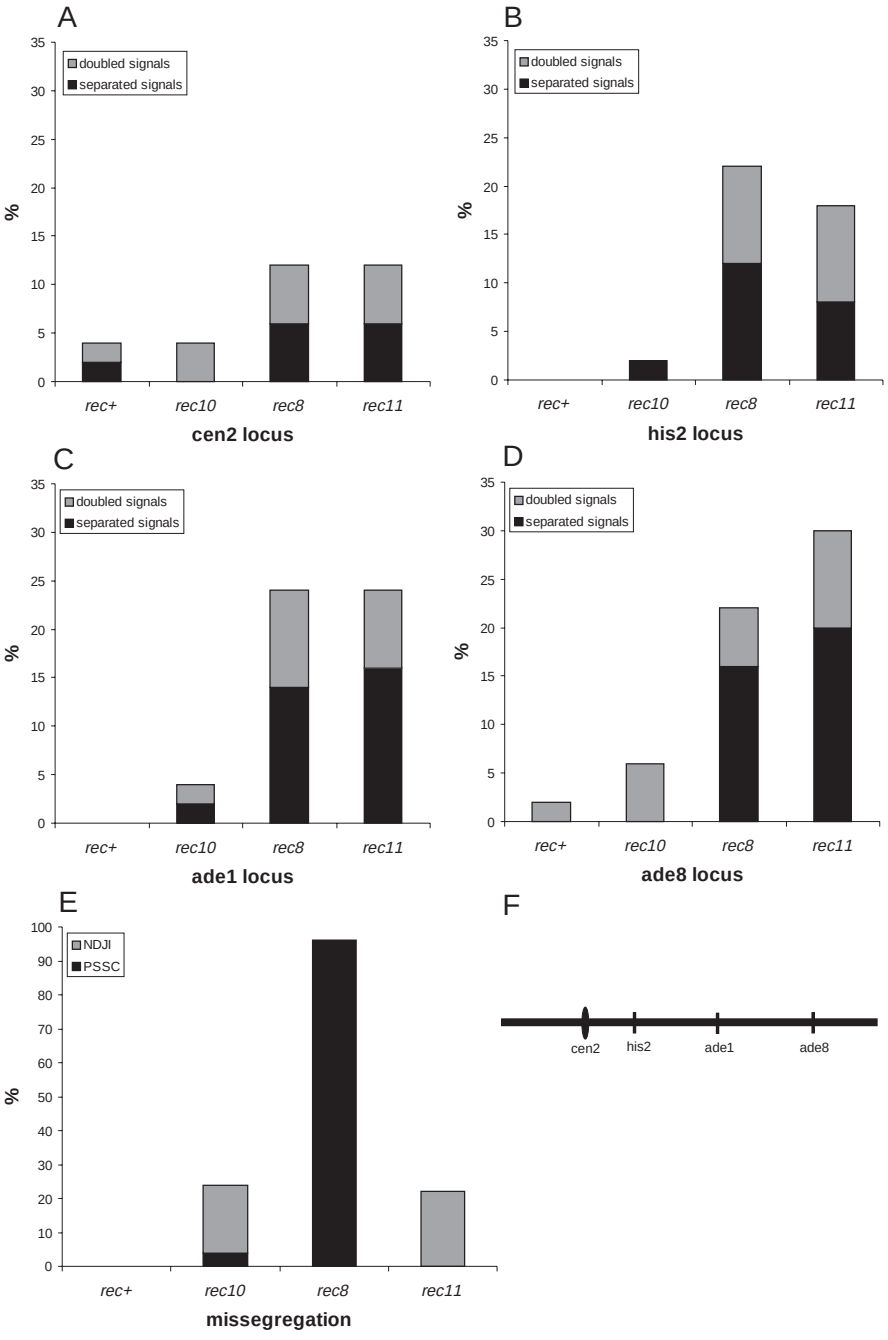

Fig. 7. Meiotic sister chromatid cohesion and chromosome segregation in the *rec10*, *rec8* and *rec11* mutants. (A-D) Sister chromatid cohesion in meiotic prophase at different loci. Heterozygous crosses were carried out with GFP-labeled strains, and the numbers of GFP signals were determined in living cells as described in Materials and Methods. 50 horse-tail nuclei were examined in each experiment. (A) Sister chromatid cohesion at the *cen2* locus. GFP labeled h^- control (AY261-1C), *rec10* (95), *rec8* (101) and *rec11* (100) strains were crossed to unlabeled h^+ control (L975), *rec10* (67), *rec8* (68-2710) and *rec11* (70) strains, respectively. (B) Sister chromatid cohesion at the *his2* locus. GFP labeled h^- control (153), *rec10* (156), *rec8* (157) and *rec11* (155) strains were crossed to unlabeled h^+ strains. The same h^+ strains were used as described for the *cen2* locus. (C) Sister chromatid cohesion at the *ade1* locus. GFP labeled h^+ control (AY234-6B), *rec10* (116), *rec8* (143) and *rec11* (117) strains were crossed to unlabeled h^- control (105), *rec10* (68), *rec8* (128) and *rec11* (132) strains, respectively. (D) Sister chromatid cohesion at the *ade8* locus. GFP labeled h^- control (AY 208-21A), *rec10* (143), *rec8* (142) and *rec11* (146) strains were crossed to unlabeled h^+ strains. The same h^+ strains were used as described for the *cen2* locus. (E) Evaluation of chromosomal mis-segregation in the *rec10*, *rec8* and *rec11* mutants. To assess PSSC (precocious sister chromatid separation), the same heterozygous crosses were carried out as described for the analysis of sister chromatid cohesion at the cen2 locus. NDJI (nondisjunction at the first division) was examined in strains bearing a homozygous GFP labeling at the *cen2* locus. Control (CT2111-2); *rec10* (119); *rec8* (161); and *rec11* (121). Cells having two nuclei were identified after Hoechst 33342 staining and the GFP signals were analyzed in 50 cells in each experiment. (F) A schematic representation of chromosome II with the positions of the GFP labeled loci along the right arm.

DSB formation (Cervantes et al., 2000; Davis and Smith, 2001), but show normal linear element morphology. In addition, meiotic breakage of chromosomes does not occur in strains lacking the *rec14* gene product (Cervantes et al., 2000; Davis and Smith, 2001), but it showed altered linear elements (Fig. 3) that differed from those in *rec12* (Fig. 2).

Conversely, although LE formation does not depend on DSB formation, some early prophase proteins influence both processes and recombination. The *rec8* and *rec10* mutants were shown to form meiotic breaks with reduced efficiency (Cervantes et al., 2000). In the cohesin mutants *rec8* (Molnar et al., 1995) and *rec11*, as well as in the double mutant *rec8rec11* (Fig. 5), identical and, from wild-type, strongly deviating LE structures were observed. In *rec10* the linear elements were missing completely (Fig. 5). Obviously cohesins and *rec10* are involved in LE and DSB formation (see below). *rec12* and *rec14* are also involved in both processes. The most striking feature of the *rec12* mutant was the abundant occurrence of nuclei with single long elements at the expense of networks and bundles (Fig. 2E). Networks and bundles are the most complicated linear element morphologies. Their rarity indicates that linear element processing is altered in the *rec12* mutant. Thus fission yeast Rec12 is similar to its budding yeast homolog in the sense that both proteins are involved in the initiation of homologous recombination and also in proper chromosome organization. However, their role in chromosome organization might be somewhat different: *spo11* null mutants are capable of forming axial elements, but exhibit severe homolog synapsis defects (Loidl et al., 1994).

The most striking feature of the *rec14* mutant was the high frequency of networks (Fig. 3). *rec14* is a functional homolog of REC103 of *S. cerevisiae* (Evans et al., 1997). Both genes were shown to be involved in early stages of meiotic recombination (Evans et al., 1997; Gardiner et al., 1997; Cervantes et al., 2000), but the known phenotypes of their mutants do not allow a clear conclusion about the function of *rec14* in linear element formation. However, it should be noted that the expression pattern of *rec14* is different from that of other recombination genes in fission yeast: its transcript is present both in meiotic and mitotically dividing cells, and the mutant shows a slow mitotic growth phenotype (Evans et al., 1997). Thus it is conceivable that the observed alteration in linear element formation is a consequence of a disturbance of basic chromosome structure not directly related to the initiation of recombination.

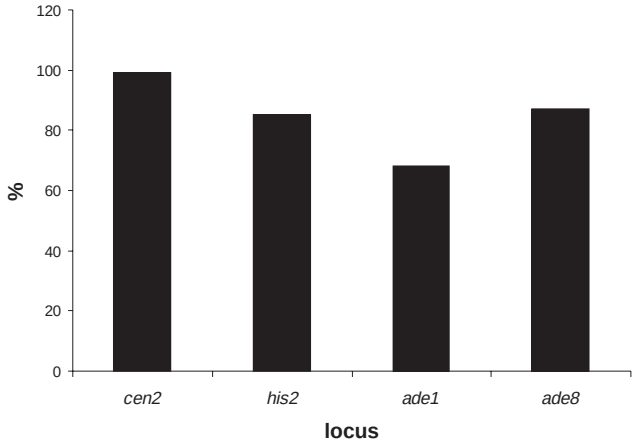

Fig. 8. Homologous chromosome pairing in the *rec10* mutant relative to wild-type. To emphasize the pairing properties of the mutant, the persentage of homologous chromosome pairing in the different chromosomal regions in *rec10* was expressed relative to that measured in the wild-type strain. (The original data are presented in Table 2.)

meu13 participates in homologous chromosome pairing in fission yeast in a recombination-independent mechanism and shows significant sequence homology to Hop2 (Nabeshima et al., 2001), a protein that ensures synapsis between homologous chromosomes in *S. cerevisiae* (Leu et al., 1998). Double-strand breaks form in *meu13* deletion strains and their repair is retarded (Shimada et al., 2002). The typical morphological change in this mutant was the frequent occurrence of network- and bundle-like structures (Fig. 4), some of which rather resembled an unspecific deposition of linear element material than a functional structure (Fig. 4A). Meu13p is localized to meiotic chromatin during the horse-tail nuclear movement stage (Nabeshima et al., 2001). Because linear elements were most aberrant at early prophase stages in the *meu13* mutant (Fig. 4A), it is suggested that Meu13 might serve as a loading site for linear element proteins. In turn, linear elements are needed to achieve the full level of meiotic chromosome pairing (Table 2; Fig. 8). Thus the decreased meiotic pairing and recombination observed in the *meu13* mutant might be a consequence of imperfect formation of linear elements.

A possible explanation for the regional specificity of recombination loss in *rec8, rec10* and *rec11* mutants

DeVeaux and Smith have observed first a regional specificity of loss of meiotic recombination in the *rec8*, *rec10* and *rec11* mutants (DeVeaux and Smith, 1994). They have found that meiotic recombination was impaired most severely in a ~2 Mb region surrounding the *ade6* locus of chromosome III, while other loci examined were less severely affected. Parisi et al. and Krawchuck et al. extended their study and showed that meiotic recombination is decreased severely in the centromeric region of each chromosome in these mutants (Parisi et al., 1999; Krawchuck et al., 1999). Based on epistasis analysis and classical chromosome segregation studies, Krawchuk et al. proposed that Rec8, Rec10 and Rec11 are involved in a 'meiotic sister chromatid cohesion pathway' and promote homologous chromosome pairing in the centromer proximal regions of chromosomes (Krawchuk et al., 1999). Our results largely confirm this hypothesis and suggest that the underlying structural reason for the regional specificity is a defect in the formation of linear elements in the *rec8*, *rec10* and *rec11* mutants.

Rec8 and Rec11 are meiotic cohesins (Watanabe and Nurse, 1999; Parisi et al., 1999; Davis and Smith, 2001). Rec8 has two different functions correlating with distinguishable localization. It was found to locate to the centromeres of chromosomes (Watanabe and Nurse, 1999) and to ensure reductional segregation at the first meiotic division (Watanabe and Nurse, 1999; Molnar et al., 2001a). In addition, Rec8 as well as Rec11 are involved in sister chromatid cohesion along the chromosome arms (Fig. 6). We have found a severe defect in linear element formation in *rec8* and *rec11* mutants (Molnar et al., 1995) (Fig. 5). Deletion of either of the meiotic cohesins

resulted in a typical morphological change observed so far only in these mutants. Moreover, the double mutant showed the same phenotype (Fig. 5). The most straightforward interpretation of these observations is that Rec8 and Rec11 work in a complex, and that functional cohesin complexes are indispensable for proper linear element formation. Cohesin complexes may serve as loading sites for linear element polymerization. A similar function of *S. cerevisiae* Rec8 for axial element formation has been suggested (Klein et al., 1999). The *rec10* mutant does not form linear element material at all, but it undergoes meiosis with similar timing and efficiency to that of a wild-type strain (Fig. 6). Direct investigation of the sister chromatid cohesion along chromosome II in the *rec10* mutant has shown that linear elements are basically dispensable for sister chromatid cohesion in fission yeast (Fig. 7).

The role of linear elements in chromosome pairing

Cells employ several mechanisms to effect chromosome pairing. The contribution of horse-tail movements and telomere clustering to homologous chromosome pairing is well-demonstrated in fission yeast (for a review, see Yamamoto and Hiraoka, 2001). The *rec10* mutant shows regular horse-tail movements (M.M., unpublished). Because mutants impaired in telomere clustering perform aberrant nuclear movement (Cooper et al., 1998; Nimmo et al., 1998; Hiraoka et al., 2000), the above observation indirectly indicates that telomere clustering is regular in *rec10*. Therefore, the decrease in chromosome pairing in the *rec10* mutant is likely to be attributable to the lack of linear elements.

The highest level of homologous chromosome contact was detected at the centromere of chromosome II, both in the control and the *rec10* mutant strains (Table 2). A similar result was obtained in a wild-type strain by fluorescence in situ hybridization experiments performed on nuclear spreads: Scherthan et al. has shown that all the centromeres form a cluster and maintain this state throughout meiotic prophase in fission yeast (Scherthan et al., 1994). This observation suggests that cells have a mechanism to accomplish the clustering of centromeres independently from linear element formation or *rec10* function. In the control strain, a gradual increase in chromosome pairing was observed towards the telomere (Table 2). This can be explained by the effect of telomere clustering, which increases the possibility of chance contacts primarily at the telomere proximal regions of chromosomes.

In the *rec10* mutant a decrease in homologous chromosome pairing was measured at each locus along the chromosome arm (Table 2). The reduction was slight at the *his2* and *ade*8 loci (Fig. 8). Among the examined loci, *ade8* is closest to the telomere and *his2* is to the centromere. Telomere clustering may promote pairing of homologous chromosomes most efficiently in the *ade8* region in absence of linear elements. The efficient clustering of centromeres in *rec10* might exert a similar supporting effect for pairing of centromere proximal loci. An alternative explanation is based on the fact that the *his2* locus is near the mating-type locus, which contains heterochromatin. Thus, fission yeast may use the heterochromatin of the mating-type and centromeres to achieve linear element independent pairing of the centromere-proximal region in this chromosome arm. The *ade1* locus is situated in the middle of the chromosome arm, and the most severe defect in chromosome pairing was detected at this locus (Fig. 8). Linear elements are thus likely to be most important for chromosome pairing at interstitial arm regions. Clustering of telomeres and centromeres provide for alignment of the telomere and centromere proximal regions, respectively. This probably ensures frequent contact of the corresponding regions, and homologous sequences may have a better chance for pairing despite the lack of chromatin organization by linear elements.

Concluding remarks

rec10-155::LEU2 is a partial deletion lacking residues 683 to 791 (Lin and Smith, 1995). This mutant undergoes meiosis similarly to wild-type, but lacks linear elements completely. This provided a good opportunity to analyze the role of linear elements in meiosis. We have found that linear elements are basically dispensable for sister chromatid cohesion, but contribute to homologous paring of chromosomes. Although we cannot rule out the possibility that *rec10* promotes homologous chromosome pairing independently from its function in linear element formation, the most straightforward interpretation of our data is that Rec10 exerts its effect on homologous chromosome pairing through its function in linear element formation. What is the role of *rec10* in linear element formation? *rec10* might encode a structural protein of linear elements. However, a regulatory role is also plausible. *rec10* may regulate linear element formation directly or through more general processes, for example, through the regulation of chromatin structure.

We thank Gerald R. Smith, Masayuki Yamamoto and Hiroshi Nojima for strains, Toni Wyler and Karl Babl for technical assistance, and Jürg Bähler and Josef Loidl for critical reading of the manuscript. This work was supported by the Swiss National Foundation (to J.K.) and the Japan Science and Technology Corporation (Y.H.).

References

Bähler, J., Wyler, T., Loidl, J. and Kohli, J. (1993). Unusual nuclear structures in meiotic prophase of fission yeast: a cytological analysis. *J. Cell Biol.* **121**, 241-256.

Bähler, J., Wu, J.-Q., Longtine, M. S., Shah, N. G., McKenzie, A., III, Steever, A. B., Wach, A., Philippsen, P. and Pringle, J. R. (1998). Heterologous modules for efficient and versatile PCR-based gene targeting in *Schizosaccharomyces pombe*. *Yeast* **14**, 943-951.

Beach, D., Rodgers, L. and Gould, J. (1985). *RAN1*$^{+}$ controls the transition from mitotic division to meiosis in fission yeast. *Curr. Genet.* **10**, 297-311.

Cervantes, M. D., Farah, J. A. and Smith, G. R. (2000). Meiotic DNA breaks associated with recombination in *S. pombe*. *Mol. Cell* **5**, 883-888.

Chikashige, Y., Ding, D.-Q., Funabiki, H., Haraguchi, T., Mashiko, S., Yanagida, M. and Hiraoka, Y. (1994). Telomere-led premeiotic chromosome movement in fission yeast. *Science* **264**, 270-273.

Chikashige, Y., Ding, D.-Q., Imai, Y., Yamamoto, M., Haraguchi, T. and Hiraoka, Y. (1997). Meiotic nuclear reorganization: switching the position of centromeres and telomeres in fission yeast *Schizosaccharomyces pombe*. *EMBO J.* **16**, 193-202.

Cooper, J. P., Watanabe, Y. and Nurse, P. (1998). Fission yeast Taz1 protein is required for meiotic telomere clustering and recombination. *Nature* **23**, 828-831.

Davis, L. and Smith, G. R. (2001). Meiotic recombination and chromosome segregation in *Schizosaccharomyces pombe*. *Proc. Natl. Acad. Sci. USA* **98**, 8395-8402.

DeVeaux, L. C., Hoagland, N. A. and Smith, G. R. (1992). Seventeen complementation groups of mutations decreasing meiotic recombination in *Schizosaccharomyces pombe*. *Genetics* **130**, 251-262.

DeVeaux, L. C. and Smith, G. R. (1994). Region-specific activators of meiotic recombination in *Schizosaccharomyces pombe*. *Genes Dev*. **8**, 203-210.

Ding, R. and Smith, G. R. (1998). Global control of meiotic recombination genes by *Schizosaccharomyces pombe rec16* (*rep1*). *Mol. Gen. Genet.* **258**, 663-670.

Egel, R. (1973). Commitment to meiosis in fission yeast. *Mol. Gen. Genet.* **121**, 277-284.

Egel, R. and Egel-Mitani, M. (1974). Premeiotic DNA synthesis in fission yeast. *Exp. Cell. Res.* **88**, 127-134.

Evans, D. H., Li, Y. F., Fox, M. E. and Smith, G. R. (1997). A WD repeat protein, Rec14, essential for meiotic recombination in *Schizosaccharomyces pombe*. *Genetics* **146**, 1253-1264.

Gardiner, J. M., Bullard, S. A., Chrome, C. and Malone, R. E. (1997). Molecular and genetic analysis of REC103, an early meiotic recombination gene in yeast. *Genetics* **146**, 1265-1274.

Gutz, H., Heslot, H., Leupold, U. and Loprieno, N. (1974). *Schizosaccharomyces pombe*. In *Handbook of Genetics*, Vol. 1 (ed. R. C. King), pp. 395-446. New York: Plenum Press.

Hiraoka, Y., Ding, D.-Q., Yamamoto, A., Tsutsumi, C. and Chikashige, Y. (2000). Chraracterization of fission yeast meiotic mutants based on live observation of meiotic prophase nuclear movement. *Chromosoma* **104**, 203-214.

Hirata, A. and Tanaka, K. (1982). Nuclear behavior during conjugation and meiosis in the fission yeast *Schizosaccharomyces pombe. J. Gen. Appl. Microbiol*. **28**, 263-274.

Keeney, S., Giroux, C. N. and Kleckner, N. (1997). Meiosis-specific DNA double-strand breaks are catalyzed by Spo11, a member of a widely conserved protein family. *Cell* **88**, 375-384.

Kleckner, N. (1996). Meiosis: how could it work? *Proc. Natl. Acad. Sci. USA* **93**, 8167-8174.

Klein, F., Mahr, P., Galova, M., Buonomo, S. B. C., Michaelis, C., Nairz, K. and Nasmyth, K. (1999). A central role for cohesins in sister chromatid cohesion, formation of axial elements, and recombination during yeast meiosis. *Cell* **98**, 91-103.

Kohli, J. (1994). Telomeres lead chromosome movement. *Curr. Biol*. **4**, 724-727.

Kohli, J. and Bähler, J. (1994). Homologous recombination in fission yeast: absence of crossover interference and synaptonemal complex. *Experientia* **50**, 296-306.

Krawchuk, M. D., DeVeaux, L. C. and Wahls, W. P. (1999). Meiotic chromosome dynamics dependent upon the *rec8*$^+$, *rec10*$^+$ and *rec11*$^+$ genes of the fission yeast Schizosaccharomyces pombe. *Genetics* **153**, 57-68.

Leu, J.-Y., Chua, P. R. and Roeder, G. S. (1998). The meiosis-specific Hop2 protein of *S. cerevisiae* ensures synapsis between homologous chromosomes. *Cell* **94**, 375-386.

Li, Y. F., Numata, M., Wahls, W. P. and Smith, G. R. (1997). Region-specific meiotic recombination in *Schizosaccharomyces pombe*: the *rec11* gene. *Mol. Microbiol*. **23**, 869-878.

Lin, Y. and Smith, G. R. (1994). Transient, meiosis-induced expression of the *rec6* and *rec12* genes of *Schizosaccharomyces pombe*. *Genetics* **136**, 769-779.

Lin, Y. and Smith, G. R. (1995). Molecular cloning of the meiosis-induced *rec10* gene of *Schizosaccharomyces pombe*. *Curr. Genet.* **27**, 440-446.

Loidl, J., Klein, F. and Scherthan, H. (1994). Homologous pairing is reduced but not abolished in asynaptic mutants of yeast. *J. Cell Biol.* **125**, 1191-1200.

Molnar, M., Bähler, J., Sipiczki, M. and Kohli, J. (1995). The *rec8* gene of *Schizosaccharomyces pombe* is involved in linear element formation, chromosome pairing and sister-chromatid cohesion during meiosis. *Genetics* **141**, 61-73.

Molnar, M., Bähler, J., Kohli, J. and Hiraoka, H. (2001a). Live observation of fission yeast meiosis in recombination-deficient mutants: a study on achiasmate chromosome segregation. *J. Cell Sci*. **114**, 2843-2853.

Molnar, M., Parisi, S., Kakihara, Y., Nojima, H., Yamamoto, A., Hiraoka, Y., Bozsik, A., Sipiczki, M. and Kohli, J. (2001b). Characterization of *rec7*, an early meiotic recombination gene in *Schizosaccharomyces pombe. Genetics* **157**, 519-532.

Moreno, S., Klar, A. and Nurse, P. (1991). Molecular genetic analysis of fission yeast *Schizosaccharomyces pombe*. *Methods Enzymol*. **194**, 795-823.

Munz, P. (1994). An analysis of interference in the fission yeast *Schizosaccharomyces pombe*. *Genetics* **137**, 701-707.

Nabeshima, K., Nakagawa, T., Straight, A. F., Murray, A., Chikashige, Y., Yamashita, Y. M., Hiraoka, Y. and Yanagida, M. (1998). Dynamics of centromeres during metaphase-anaphase transition of fission yeast: Dis1 is implicated in force balance in metaphase bipolar spindle. *Mol. Biol. Cell* **9**, 3211-3225.

Nabeshima, K., Kakihara, Y., Hiraoka, Y. and Nojima, H. (2001). A novel meiosis- specific protein of fission yeast, Meu13p, promotes homologous pairing independently of homologous recombination. *EMBO J*. **20**, 3871-3881.

Nimmo, E. R., Pidoux, A. L., Perry, P. E. and Allshire, R. C. (1998). Defective meiosis In telomere-silencing mutants of *Schizosaccharomycs pombe*. *Nature* **23**, 825-828.

Olson, L. W., Eden, U., Egel-Mitani, M. and Egel, R. (1978). Asynaptic meiosis in fission yeast? *Hereditas* **89**, 189-199.

Parisi, S., McKay, M. J., Molnar, M., Thompson, M. A., van der Speck, P. J., van Drunnen-Schoenmaker, E., Kanaar, R., Lehmann, E., Hoeijmakers, J. H. J. and Kohli, J. (1999). Rec8p, a meiotic recombination and sistercohesion phosphoprotein of the Rad21p family conserved from fission yeast to human. *Mol. Cell. Biol*. **19**, 3515-3528.

Ponticelli, A. S. and Smith, G. R. (1989). Meiotic recombination-deficient mutants of *Schizosaccharomyces pombe*. *Genetics* **123**, 45-54.

Robinow, C. F. (1977). The number of chromosomes in *S. pombe*: light microscopy of stained preparations. *Genetics* **87**, 491-497.

Roeder, G. S. (1997). Meiotic chromosomes: it takes two to tango. *Genes Dev.* **11**, 2600-2621.

Scherthan, H., Bähler, J. and Kohli, J. (1994). Dynamics of chromosome organization and pairing during meiotic prophase of fission yeast. *J. Cell. Biol*. **127**, 273-285.

Shimada, M., Nabeshima, K., Tougan, T. and Nojima, H. (2002). The meiotic recombination checkpoint is regulated by checkpoint *rad*$^+$ genes in fission yeast. *EMBO J.* **21**, 2807-2818.

Shimanuki, M., Miki, F., Ding, D.-Q., Chikashige, Y., Hiraoka, Y., Horio, T. and Niwa, O. (1997). A novel fission yeast gene, *kms1*$^+$, is required for the formation of meioticprophase-specific nuclear architecture. *Mol. Gen. Genet* **254**, 238-249.

Sugiyama, A., Tanaka, K., Okazaki, K., Nojima, H. and Okayama, H. (1994). A zinc finger protein controls the onset of premeiotic DNA synthesis of fission yeast in a Mei2-independent cascade. *EMBO J*. **13**, 1881-1887.

Watanabe, Y. and Nurse, P. (1999). Cohesin Rec8 is required for reductional chromosome segregation at meiosis. *Nature* **400**, 461-464.

Watanabe, Y., Iino, Y., Furuhata, K., Shimoda, C. and Yamamoto, M. (1988). The *S. pombe mei2* gene encoding a crucial molecule for commitment to meiosis is under the regulation of cAMP. *EMBO J.* **7**, 761-767.

Yamamoto, A. and Hiraoka, Y. (2001). How do meiotic chromosomes meet their homologous partner? Lessons from fission yeast. *BioEssays* **23**, 526-533.

Yamamoto, A., West, R. R., McIntosh, J. R. and Hiraoka, Y. (1999). A cytoplasmic dynein heavy chain is required for oscillatory nuclear movement of meiotic prophase and efficient meiotic recombination in fission yeast. *J. Cell Biol*. **145**, 1233-1249.

Young, J. A., Schreckhise, R. W., Steiner, W. W. and Smith, G. R. (2002). Meiotic recombination remote from prominent break sites in *S. pombe*. *Mol. Cell* **9**, 253-263.

Zickler, D. and Kleckner, N. (1999). Meiotic chromosomes: integrating structure and function. *Annu. Rev. Genet.* **33**, 603-754.